Scholarly Research Journal for Humanity Science & English Language,
Online ISSN 2348-3083, SJIF 2016 = 4.44, www.srjis.com
UGC Approved Sr. No.48612, AUG-SEPT 2017, VOL- 4/23

A LOW-COST FOUR-LED OPTICALLY STIMULATED LUMINESCENCE READER WITH PHOTODIODE-STABILIZED BLUE STIMULATION AND PMT CURRENT-MODE DETECTION

A. A. Chaudhary
Institute of Science, Nagpur, Maharashtra, India
Email: *saifeeabdul1973@gmail.com*

Abstract

Optically stimulated luminescence (OSL) readers are central to radiation dosimetry and luminescence dating, yet commercial systems cost roughly 12 lakhs to 40 lakh (Indian rupees) and are difficult to modify. We describe the design and construction of a compact continuous-wave OSL (CW-OSL) reader assembled from locally sourced parts. Four high-power blue LEDs (peak emission 450 nm) are focused on a powder or pellet sample and deliver 3.7×10^{-5} W cm^{-2} at a drive power of 95 mW; a photodiode feedback loop stabilizes the LED output. Luminescence is detected by a head-on Hamamatsu R1387 photomultiplier tube (PMT) operated at 750 V behind a UV-pass filter, and the PMT current is read by a Pico ammeter, buffered, digitized by the 12-bit ADC of an STM32F103C8T6 (ARM Cortex-M3) microcontroller and passed to a PC. We give the optical layout, the electronic design, first-order design equations for stimulation photon flux, PMT gain and loop stabilization, and a specification-level comparison with the Risø DA-20 and Nucleonics TOSL-1008 readers. The reader is simple, modular and inexpensive, but its stimulation power density is about three orders of magnitude below that of commercial units, which confines it to slow-decay CW-OSL work; the consequences and the upgrade path are discussed.

Keywords: *optically stimulated luminescence; OSL reader; photomultiplier tube; blue LED; feedback stabilization; low-cost instrumentation*

1 Introduction

In OSL, a previously irradiated insulator or wide-gap semiconductor is illuminated with light of a fixed wavelength. The light releases charge carriers from radiation-induced traps; their recombination at luminescence centers produces emission whose time-integrated intensity scales with the absorbed dose [1, 2]. Because readout is done at room temperature, OSL avoids the thermal quenching and heating hardware of thermoluminescence (TL) and permits repeated readouts and automation. OSL is now used in personal, environmental, medical and retrospective dosimetry and in optical dating of sediments [3, 4].

For a first-order process with negligible retrapping and constant stimulation, the OSL intensity decays exponentially,

$$I(t) = n_0\, \sigma\varphi\, e^{-\sigma\varphi t} = I_0\, e^{-t/\tau},\quad T = \frac{1}{\sigma\varphi} \qquad (1)$$

where n_0 is the initial trapped-charge concentration, σ the photo-ionization cross-section at the stimulation wavelength and φ the stimulation photon flux (photons cm^{-2} s^{-1}). The area under $I(t)$ equals n_0 and therefore measures dose; the decay constant τ depends inversely on the stimulation intensity. A reader must therefore (i) deliver a known, stable φ, (ii) separate the weak luminescence from scattered stimulation light, and (iii) record $I(t)$ with adequate time resolution and dynamic range.

Commercial readers such as the Risø DA-20 and the Nucleonics TOSL-1008 satisfy these requirements [5, 6, 7, 8] but cost about 30 lakh to 40 lakh and 12 lakh to 20 lakh, respectively, and depend on vendor service. Laboratory-built integrated TL/OSL systems have been reported [9], but designs that are fully documented, PC-controlled and based on inexpensive, widely available electronics remain scarce. Here we describe such a reader: a four-LED blue CW-OSL system with photodiode-stabilized stimulation and current-mode PMT detection, controlled by a low-cost ARM Cortex-M3 board. The present paper gives the design in full.

2 Instrument design

2.1 Architecture

Figure 1 shows the functional blocks. The OSL assembly houses the sample, the LED cluster, a stimulation-monitor photodiode and the PMT. The PMT is biased by a regulated high-voltage (HV) supply set to 750 V; its anode current is measured by a digital Pico ammeter, inverted and buffered, and digitized by the STM32F103C8T6 ("Blue Pill" board). A GPIO pin (PB9) drives an opto-isolated relay that switches the LED control circuit, so that stimulation starts and stops under program control. The LED control circuit contains the photodiode feedback loop (Sect. 2.3).

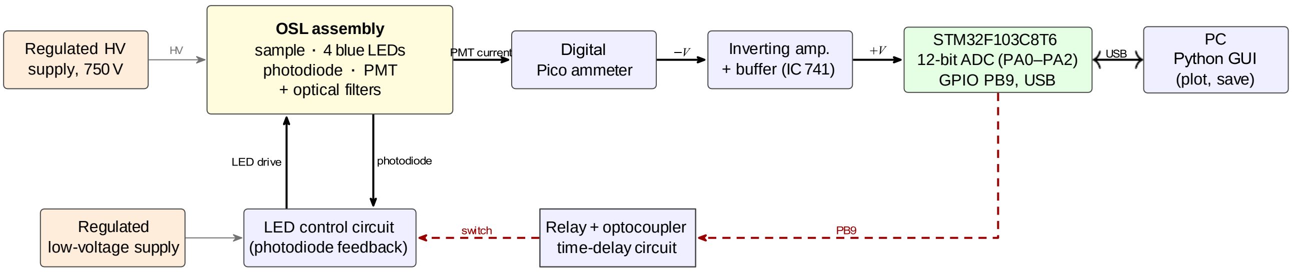

Figure 1. Block diagram of the OSL reader. Solid arrows: signal path; dashed red arrows: program control; thin arrows: power. The LED–photodiode–control loop stabilizes the stimulation intensity.

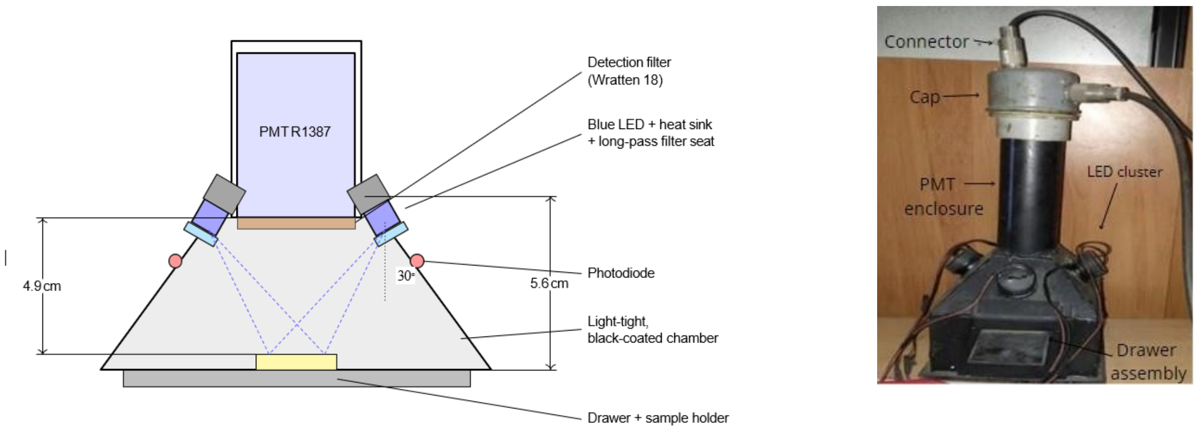

(a) **(b)**

Figure 2. Optical assembly. (a) Schematic cross-section (not to scale; two of the four LED channels shown; dimensions from the construction drawings). The LED axes make 30° with the vertical, the PMT window is 4.9 cm above the sample and the LED filter seats are 4.8 cm from it. (b) Photograph of the PMT enclosure, LED cluster and drawer.

2.2 Sample chamber and optical layout

The chamber is cut from hard foam sheet in the form of a trapezoidal frustum (bases 4.4 and 12.6 cm, height 5.6 cm) and coated internally and externally with matt black paint to suppress reflections and stray light (Fig. 2). A plastic drawer sliding in grooves carries a cylindrical sample holder (height 0.5 cm, volume 1.57 cm^3) that receives powder or pellets. Four LED holders (channels) are fitted on the four inclined faces; each LED, with its own heat sink, is aimed at the sample

at 30° to the vertical axis, with a filter seat 4.8 cm from the sample. The PMT enclosure (a 15 cm plastic pipe of 4.2 cm inner diameter) is mounted at the top center, with the PMT window 4.9 cm above the sample. A UV-pass detection filter
(Kodak Wratten 18) sits directly in front of the PMT window to reject scattered blue light while transmitting near-UV luminescence; a long-pass filter seat (e.g. Schott GG 455, 12.5 mm) is provided in each LED channel. Table 1 lists the main specifications.

2.3 Stimulation source

Spectrum and intensity. The LEDs emit a single band peaking at 450 nm with a full width at half maximum of roughly 20–25 nm (Fig. 3). With the cluster on, the intensity at the sample was measured with a digital lux meter (Metrix LX1330A+) as 9.37×10^{-6} W cm^{-2} per LED and 3.7×10^{-5} W cm^{-2} for the four LEDs together at the 95 mW setting;
the four intensities add, $\varphi_{e,\text{cluster}} = \sum^4 \varphi_{e,i} \approx 4 \times 9.37$ μWcm^{-2}. Table 2 gives the four available settings. Over these
points the per-LED intensity is well described by φ_e [μWcm^{-2}] $\approx 0.148\,P$ [mW] $- 3.9$ ($r^2 = 0.98$, four points; our fit to the tabulated data), i.e. slightly super-linear in P, possibly reflecting the LED drive characteristics.

For use in Eq. (1) the energy flux φ_e is converted to a photon flux,

$$\varphi = \frac{\varphi e\,\lambda}{hc} \tag{2}$$

At $\lambda = 450$ nm the photon energy is 2.76 eV, so $\varphi_e = 3.7 \times 10^{-5}$ W cm^{-2} corresponds to $\varphi \approx 8 \times 10^{13}$ photons cm^{-2} s^{-1}.

Intensity stabilization. LED output varies with junction temperature and with small drifts in drive current. Temperature is limited by an individual heat sink on each LED; drive-current drift is suppressed by the loop of Fig. 3. Light from the cluster generates a photodiode signal that is amplified and compared with a set point of about 3 V; the comparator output

Table 1. Main specifications of the reader. Subsystem Specification

Chamber	Hard-foam frustum, bases 4.4/12.6 cm, height 5.6 cm; sliding drawer; sample holder 0.5 cm high,
	1.57 cm^3
Stimulation	4 high-power blue LEDs, peak 450 nm; 3.7×10^{-5} W cm^{-2} at the sample (cluster, 95 mW setting), adjustable (Table 2); axes at 30° to vertical
Intensity control	Photodiode + two-stage op-amp comparator (set point ≈3 V) driving an NPN transistor with 100 Ω emitter resistor
Detector	Hamamatsu R1387 head-on PMT, 10 dynodes, multialkali cathode, 300–850 nm, borosilicate window, 38 mm; HV 750 V
Divider chain	Eleven 470 kΩ resistors (5.17 MΩ total)
Detection filter	Kodak Wratten 18 (UV-pass)
Current readout	Pico ammeter with FET-input electrometer (AD549), accuracy 0.2 % on all ranges, 1 pA lowest range resolution, USB interface
Conditioning capacitor	Unity-gain inverter and voltage follower (IC 741), 0.01 μF noise-decoupling
Controller	STM32F103C8T6, ARM Cortex-M3, 72 MHz, 12-bit ADC, 64 kB flash,
	20 kB RAM, USB 2.0 FS Host software Python GUI

Table 2. Stimulation settings. Power and per-LED intensity are as measured/tabulated for the reader; the cluster value is the sum of four equal LEDs. Photon flux from Eq. (2) at 450 nm.

LED power P (mW)	Intensity per LED (μW cm^{-2})	Cluster intensity (μW cm^{-2})	Cluster photon flux (10^{13} cm^{-2} s^{-1})
126	15.18	60.7	13.8
95	9.37	37.5	8.5
76	7.3	29.2	6.6
58	5.1	20.4	4.6

changes the base drive of the driver transistor, and hence the LED current, in the direction that restores the set intensity. In the emitter-follower stage the total LED current is $I_{LED} \simeq (V_B - V_{BE})/R_E$ with R_E = 100 Ω. For a loop with amplifier gain A, driver transconductance g_m, LED efficiency η and photodiode-stage gain k, the loop gain is $T = Ag_m \eta k$ and a fractional intensity drift δ_{ol} of the uncontrolled source is reduced to

$$\delta_{cl} = \frac{\delta_{ol}}{1+T} \tag{3}$$

Equation (3) is the standard first-order result for negative feedback; it shows what the loop can achieve but does not replace a measurement. A long-term photodiode-monitored stability test of the LED output is not part of the present data set and should accompany the design in future work.

Driving headroom. From the schematic in Fig. 3b, the 9 V rail and the 100 Ω emitter resistor limit the total LED current to well below 100 mA, whereas four 1 W blue LEDs are typically driven at a few hundred mA each. The reader therefore operates its LEDs far below their rated power (settings of 58–126 mW), and a higher-current driver is the most direct route to a higher stimulation intensity.

2.4 Luminescence detection

PMT and biasing. The R1387 is a head-on, ten-stage tube with a multialkali photocathode (300–850 nm; cathode sensitivity 80 μA/lm as listed by the manufacturer; Table 1). A 750 V supply is applied across a divider of eleven 470 kΩ resistors, giving a divider current

$$I_b = \frac{V_{HV}}{11R} = \frac{750\ \text{V}}{5.17\ \text{M}\Omega} \approx 145\ \mu\text{A}, \tag{4}$$

which exceeds the anode current in normal use (the manufacturer's maximum average anode current is 0.2 mA) by a comfortable margin so that inter-dynode voltages stay nearly constant. With secondary-emission ratio δ per stage, the current gain of an n-stage tube is

$$G = \delta^n. \tag{5}$$

The quoted overall gain of 10^5–10^7 for n = 10 corresponds to $\delta \approx$ 3.2–5.0. The anode current for a detected photon rate $\dot{N}$ and cathode quantum efficiency η_c is $I_a = e\,G\eta_c\,\dot{N}$ (current mode), where e is the electronic charge [10]. Since G depends strongly on the supply voltage (typically $G \propto V^{\alpha n}$ with $\alpha \approx$ 0.7–0.8 [10]), the HV supply stability is critical.

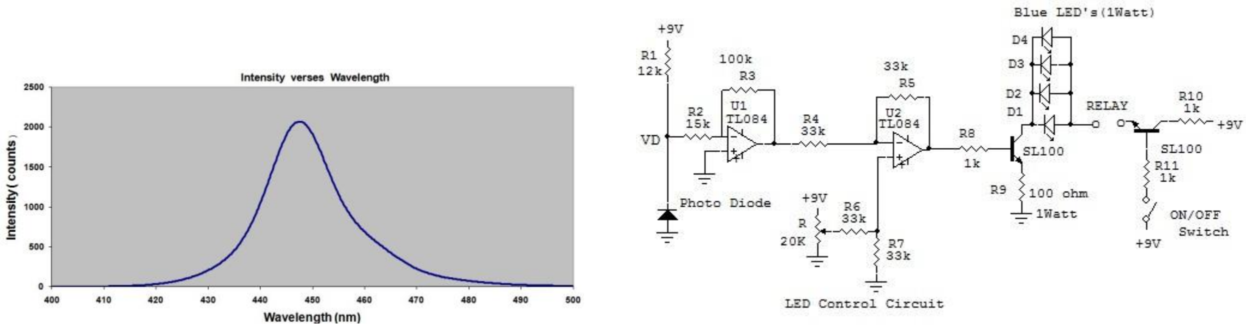

(a) (b)

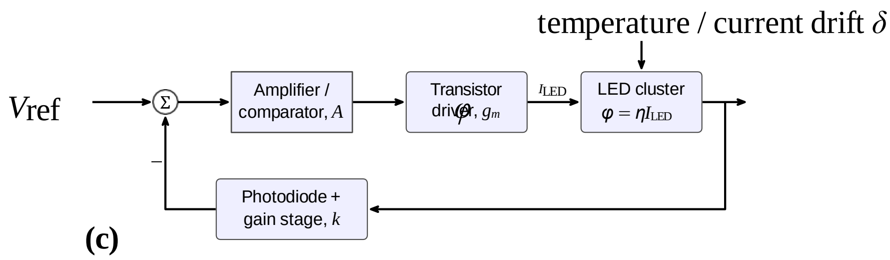

(c)

Figure 3. Stimulation source. (a) Emission spectrum of the blue LED (peak ≈450 nm; ordinate in counts). (b) LED control circuit as built: the photodiode signal is amplified (TL084) and compared with a trimmer-set reference in a second stage, which drives an SL100 transistor feeding four 1 W blue LEDs through a 100 Ω emitter resistor. (c) Equivalent negative-feedback loop.

Spectral separation. The OSL of the LiF-based phosphors studied here lies at about 350–400 nm, while the stimulation light is at 450 nm. The Wratten 18 filter in front of the PMT transmits the near-UV band and blocks the blue stimulation light, and the R1387 response (near its maximum at 420 nm and extending from 300 nm) covers the signal band.

Pico ammeter and signal conditioning. The PMT anode is connected by BNC to a digital Pico ammeter built around an FET-input electrometer amplifier (AD549); it has multiplier ranges from ×1 to $\times 10^5$, 0.2 % accuracy and 1 pA resolution on its most sensitive range. Its output is a negative voltage, which a unity-gain inverting stage (10 kΩ/10 kΩ, IC 741) converts to a positive one; a following voltage follower matches the impedance of the ADC input, and a small capacitor across the output suppresses noise. The calibrated transfer characteristic is 1 V per nA.

2.5 Control electronics

The STM32F103C8T6 (Blue Pill) reads the conditioned voltage with its 12-bit ADC and communicates with the PC over USB. Its output pin PB9 drives an EL817 optocoupler whose phototransistor turns on a BC547 that energizes a relay (with a Zener protection diode across the coil); the relay contacts switch the LED control circuit, so that stimulation begins after a programmable delay and ends at the programmed acquisition time. Optical isolation keeps relay-coil transients away from the microcontroller and the analog signal chain.

3 Comparison with commercial readers and limitations

Table 3 compares the specifications reported for the two readers most used in India [7, 8] with the present instrument. Two points stand out. First, the reader is at least 40 times cheaper than commercial readers, as reported by the authors; an itemized bill of materials should be added to substantiate the figure. Second, the blue stimulation intensity is about $80\ \mathrm{mWcm^{-2}}/0.037\ \mathrm{mWcm^{-2}} \approx 2\times10^3$ times lower than the Risø figure, corresponding to a photon-flux ratio of about
2×10^3 (from Eq. (2): 1.9×10^{17} vs. $8\times10^{13}\ \mathrm{cm^{-2}\ s^{-1}}$). By Eq. (1), decay constants scale as $1/\varphi$, so components that
decay in seconds on a commercial reader at full power would take minutes to hours here. The reader is therefore suited to
slow-decaying phosphors, teaching and method development, rather than to fast-decaying natural quartz.

Further limitations should be kept in view. (i) The stimulation intensities in Table 2 were measured with a photometric (lux) meter; converting illuminance to radiometric power at 450 nm requires the spectral response of the meter, so the absolute values are indicative and should be verified with a calibrated radiometer or photodiode. (ii) The foam chamber
is not vacuum-tight and has no inert-gas flush, thermal control or sample changer. (iii) Current-mode detection is less sensitive than photon counting at very low light levels. (iv) The 12-bit ADC sets a current resolution of ≈0.8 pA at the calibrated Pico ammeter gain

Table 3. Specification-level comparison. Commercial data as reported in the manufacturers' descriptions [7, 8]; "n.s." = not stated.

Specification	**Risø DA-20**	**Nucleonics TOSL-1008**	**This work**
Approx. cost (lakh)	30–40	12–20	≥40×lower (reported)
Blue LED peak	470 nm (20 nm band)	465 nm (460–470 nm)	450 nm
Blue intensity at sample	80 mW cm^{-2}	n.s. (3 W LEDs, 30 mW radiometric at 700 mA)	0.037mWcm^{-2}
Other wavelengths	Green 525, IR 850 nm	Green 525nm	none(blue only)
Stimulation modes	CW,LM,pulsed	CW, LM	CW(LM possible by driver modification)
Detector	25 mm bialkali PMT (EMI 9235QB), photon counting	25 mm PMT, photon counting	38mm multialkali PMT (R1387), current mode
Detection filter	Hoya U-340 (options)	n.s.	Wratten 18
Samples per run	48 (automatic changer)	single cup/planchet	1 (manual drawer)
Heating	to 700 ◦C	to 500 ◦C	none
Irradiation	90Sr/90Y β , α, X-ray	n.s.	none (external 60Co)
Control/interface	Risø software suite	Windows software, RS-232/USB	Python GUI over USB

4 Conclusions

We have described a modular, PC-controlled CW-OSL reader in which a four-LED blue source with photodiode feedback, an R1387 PMT with UV-pass filtering, a Pico ammeter and an ARM Cortex-M3 board replace the far costlier stimulation, detection and control units of commercial systems. The design equations and specifications given here allow the instrument to be reproduced and modified. The main weakness is the low stimulation intensity ($\approx 2 \times 10^3$ times below a commercial blue unit), for which a higher-current LED driver, more efficient optics and a stability test of the feedback loop are the natural next steps. Multi-wavelength stimulation, linear-modulation (LM-OSL) operation and a multi-sample changer can be added within the same architecture.

References

L. Bøtter-Jensen, S. W. S. McKeever, A. G. Wintle, Optically Stimulated Luminescence Dosimetry, Elsevier, Amsterdam (2003).

E. G. Yukihara, S. W. S. McKeever, Optically Stimulated Luminescence: Fundamentals and Applications, Wiley, Chichester (2011).

*D. J. Huntley, D. I. Godfrey-Smith, M. L. Thewalt, Optical dating of sediments, Nature **313** (1985) 105–107.*

*E. G. Yukihara, S. W. S. McKeever, Optically stimulated luminescence (OSL) dosimetry in medicine, Phys. Med. Biol. **53** (2008) R351.*

L. Bøtter-Jensen, E. Bulur, G. A. T. Duller, A. S. Murray, Advances in luminescence instrument *systems, Radiat. Meas.* ***32*** *(2000) 523–528.*

L. Bøtter-Jensen, C. E. Andersen, G. A. T. Duller, A. S. Murray, Developments in radiation, stimulation and observation facilities in luminescence measurements, Radiat. Meas. ***37*** *(2003) 535–541.*

TL/OSL Risø DA-20 reader, Technical University of Denmark (Nutech), https: //vvv. nutech. dtu. dk (manufacturer informa-tion).

Nucleonix Systems, TL/OSL reader TOSL-1008, https: //vvv. nucleonix. con (manufacturer information).

M. S. Kulkarni, D. R. Mishra, D. N. Sharma, A versatile integrated system for thermoluminescence and optically stimulated luminescence measurements, Nucl. Instrum. Methods B ***262*** *(2007) 348–356.*

Hamamatsu Photonics K.K., Photomultiplier Tubes: Basics and Applications, 3rd ed., Hamamatsu (2007).